Borneo Journal of Pharmacy
Vol 9 Issue 2 June 2026
Pages 198 – 212

https://journal.umpr.ac.id/index.php/bjop/article/view/9720
DOI: https://doi.org/10.33084/bjop.v9i2.9720
e-ISSN: 2621-4814

Research Article

In Silico Evaluation of Kaempferol, Gallic Acid, and Stigmasterol from *Lagerstroemia speciosa* as Multi-Target Antidiabetic Agents: Molecular Docking and Dynamics Simulation Study

Aditya Maulana Perdana Putra [1]
Catherina Adeline Kurniawan [1]
Anna Khumaira Sari [2]
Nabila Hadiah Akbar [2]
Khoirunnisa Muslimawati [2]
Okta Muthia Sari [1]
Dita Ayulia Dwi Sandi [1]
Normaidah [2*]
Putri Helena Junjung Buih [2]
Ariranur Haniffadli [3,4]

[1] Department of Pharmacy, Universitas Lambung Mangkurat, Banjarbaru, South Kalimantan, Indonesia
[2] Department of Professional Pharmacy Education, Universitas Lambung Mangkurat, Banjarbaru, South Kalimantan, Indonesia
[3] Korean Convergence Medical Science Major of Korea Institute of Oriental Medicine, University of Science and Technology, Daejeon, Daejeon, South Korea
[4] Herbal Medicine Resources Research Center, Korea Institute of Oriental Medicine, Naju, Jeollanam, South Korea

*email: normaidah@ulm.ac.id; phone: +6285248257718

Keywords:
Antidiabetic
Kaempferol
Lagerstroemia speciosa
Molecular dynamics

Abstract

Diabetes mellitus (DM) is a chronic metabolic disorder that leads to severe complications and continues to increase in prevalence worldwide. Although *Lagerstroemia speciosa* is a well-recognized antidiabetic medicinal plant, most *in silico* studies have focused exclusively on its major constituent, leaving the antidiabetic potential of its other phytochemicals largely unexplored. This study investigated the multi-target antidiabetic potential of phytochemicals derived from *L. speciosa* leaves using an *in silico* approach targeting three key enzymes: aldose reductase, glucokinase, and glycogen synthase kinase 3-beta (GSK3-β). A total of 62 compounds were screened by molecular docking with AutoDock Vina, followed by toxicity predictions using ProTox-II and ToxTree. The top ligand for each target, kaempferol (aldose reductase), gallic acid (glucokinase), and stigmasterol (GSK3-β), was selected for further evaluation through molecular dynamics simulations using GROMACS 2016.3 for 100 ns. Structural and interaction stability were assessed through RMSD, RMSF, SASA, Rg, and RDF analyses. Binding free energies were calculated using the MM/PBSA method via g_mmpbsa. The results indicated that stigmasterol exhibited the most favorable MM/PBSA binding free energy (–133.377 kJ/mol), followed by kaempferol (–65.714 kJ/mol) and gallic acid (–45.629 kJ/mol). However, this favorable energy was dominated by nonspecific van der Waals contributions, consistent with the diffuse interaction patterns and low hydrogen-bond occupancy (4.24%) for stigmasterol. Kaempferol exhibited the highest hydrogen-bond occupancy (64.38%), indicating a stable, consistent interaction with its target enzyme. Rg and RDF analyses confirmed the compactness and specific atomic interactions of the kaempferol and gallic acid complexes.

Received: April 30th, 2025
1st Revised: August 25th, 2025
Accepted: June 10th, 2026
Published: June 30th, 2026

INTRODUCTION

Diabetes mellitus (DM) is a chronic and increasingly prevalent metabolic disease that poses significant challenges to global health systems, affecting populations across all age groups and socioeconomic levels[1]. In Indonesia, DM is particularly concerning, with an estimated 19.5 million people diagnosed and a projected annual increase of approximately 46% in

How to cite: Putra AMP, Kurniawan CA, Sari AK, Akbar NH, Muslimawati K, Sari OM, et al. In Silico Evaluation of Kaempferol, Gallic Acid, and Stigmasterol from Lagerstroemia speciosa as Multi-Target Antidiabetic Agents: Molecular Docking and Dynamics Simulation Study. Borneo J Pharm. 2026;9(2):198-212. doi:10.33084/bjop.v9i2.9720

prevalence. The chronic progression of DM is associated with serious complications, including retinopathy, nephropathy, neuropathy, and an elevated risk of cardiovascular disease[2].

Despite the availability of various antidiabetic medications, many current treatments are limited by adverse effects, poor patient adherence, and declining efficacy over time. These challenges underscore the need for novel, safer, and more effective therapeutic agents. Because diabetes mellitus arises from multiple interconnected metabolic pathways, single-target agents often have limited efficacy; therefore, multi-target strategies that simultaneously modulate multiple enzymes involved in glucose metabolism are increasingly pursued in antidiabetic drug discovery[3,4]. In this context, computational drug discovery approaches, such as molecular docking and molecular dynamics (MD) simulations, have emerged as powerful tools. These *in silico* methods enable rapid, cost-effective screening of bioactive compounds and allow dynamic analysis of protein–ligand interactions under near-physiological conditions[5,6]. Molecular docking, in particular, has been widely used in antidiabetic drug research to target key enzymes involved in glucose metabolism[7].

Aldose reductase, glucokinase, and glycogen synthase kinase 3-beta (GSK3-β) are three critical enzymes implicated in the pathophysiology of diabetes. Aldose reductase is a rate-limiting enzyme in the polyol pathway, in which excess glucose is converted to sorbitol, contributing to oxidative stress and diabetic complications[8]. Glucokinase plays a central role in glucose homeostasis by catalyzing the phosphorylation of glucose to glucose-6-phosphate, serving as a glucose sensor in pancreatic β-cells[9]. GSK3-β is involved in insulin signaling and glycogen metabolism; its overactivation is associated with insulin resistance and impaired glycogen synthesis[10]. Targeting these enzymes may help regulate blood glucose levels and mitigate the progression of diabetes-related complications.

Lagerstroemia speciosa (L.) Pers., commonly known as the Bungur plant, is a medicinal species native to Southeast Asia and traditionally used to treat various ailments, including diabetes, kidney stones, and hypertension[11]. Previous studies have identified corosolic acid as the major bioactive compound in *L. speciosa*, exhibiting a wide spectrum of pharmacological activities, such as antidiabetic, antioxidant, anti-inflammatory, and anticancer effects[12]. Additionally, the plant's leaves contain diverse phytochemicals, including triterpenes, ellagitannins, flavonoids, tannins, and glycosides, which may synergistically contribute to its therapeutic potential[13,14]. However, most *in silico* investigations of *L. speciosa* have focused narrowly on corosolic acid, leaving other potentially active constituents underexplored[15,16].

This study aims to address this research gap by conducting a comprehensive *in silico* evaluation of 62 phytochemicals derived from *L. speciosa*. Using molecular docking, we screened these compounds for their binding affinity to aldose reductase, glucokinase, and GSK3-β. The top candidate for each target was further analyzed using 100 ns MD simulations to assess the dynamic behavior and stability of the resulting complexes. Additionally, binding free energy calculations using the Molecular Mechanics/Poisson–Boltzmann Surface Area (MM/PBSA) method were performed to quantify the strength of protein–ligand interactions.

MATERIALS AND METHODS

Materials

This study employed an integrated *in silico* framework to identify, evaluate, and optimize potential small-molecule antagonists derived from *L. speciosa* targeting three key diabetic enzymes: aldose reductase, glucokinase, and GSK3-β. Computational modeling, molecular docking, and trajectory post-processing were executed on a dedicated Linux workstation running Ubuntu 23.04.5 LTS. The system hardware comprised an Intel Core i5-11400 processor (12 MB cache, up to 4.40 GHz), an NVIDIA GeForce GTX 1080 Ti graphics processing unit (11 GB VRAM), 64 GB of system RAM, a 256 GB SATA hard disk drive, and a 256 GB NVMe solid-state drive for accelerated trajectory read/write operations.

Methods

Biomolecular targets and phytochemical library retrieval

Three-dimensional crystallographic structures of the target proteins were retrieved from the RCSB Protein Data Bank (http://www.rcsb.org/pdb/): human aldose reductase in complex with inhibitor (PDB ID: 3S3G), human glucokinase (PDB ID: 6E0I), and human GSK3-β (PDB ID: 1Q5K). A curated library of 62 bioactive phytochemicals reported in *L. speciosa* was compiled from the published literature[13,17,18]. Chemical structures, canonical Simplified Molecular Input Line-Entry

System (SMILES) strings, and 3D SDF files were obtained from the NCBI PubChem database (http://pubchem.ncbi.nlm.nih.gov/). The complete list of test compounds is compiled in **Table I**.

Table I. Curated phytochemical library derived from *L. speciosa*.

Code	Compound Name	Code	Compound Name
1	γ-Sitosterol	32	Neophytadiene
2	Oleamide	33	2-Pentadecanone
3	cis-11-Eicosenamide	34	Heptadecane
4	Hexadecanamide	35	Oleic acid
5	Octadecanamide	36	Cyclononanone
6	Stigmasterol	37	9,12-Octadecadienoic acid
7	Glycerol β-palmitate	38	Octadecanoic acid
8	Squalene	39	Linolenic acid
9	*n*-Hexadecanoic acid	40	Diacetonyl
10	Phytol	41	Stigmastan-3,5-diene
11	Campesterol	42	Diamyl phthalate
12	Vitamin E (2H-1-Benzopyran-6-ol)	43	Cyclononasiloxane
13	Phytol acetate	44	Cyclotetracosane
14	Ethyl α-D-glucopyranoside	45	9,19-Cyclolanostan-3-ol
15	3,7,11,15-Tetramethyl-2-hexadecen-1-ol	46	Z-5-Nonadecene
16	1,2,3-Benzenetriol	47	1-Heneicosyl formate
17	17-Pentatriacontene	48	1-Hexacosanol
18	2-Methoxy-4-vinylphenol	49	Stachyurin
19	Cholesta-4,6-dien-3-ol	50	2,3-(*S*)-Hexahydroxydiphenoyl-D-glucose
20	1,2-Propanediol	51	Casuarinin
21	1(10),3-Dien-17-yl acetate	52	Ellagic acid
22	α-Hydroxymyristic acid	53	Corosolic acid
23	Lageracetal	54	Gallic acid
24	Stigmast-5-en-3-ol oleate	55	4-Hydroxybenzoic acid
25	α-Tocopherolquinone	56	Caffeic acid
26	Octadecane	57	p-Coumaric acid
27	Pentacosane	58	Kaempferol
28	Dodecane	59	Quercetin
29	Tetracosane	60	Isoquercitrin
30	Tricosane	61	Maslinic acid
31	Docosane	62	Pterocarinin

Molecular software suite

Structure drawing, energy minimization, and format conversions were performed using ChemDraw Professional 18.2. Pharmacokinetic profiling and toxicity screenings were carried out using the SwissADME web server (http://www.swissadme.ch) and the ProTox-II platform (https://tox-new.charite.de/) alongside ToxTree software. Molecular docking simulations were conducted using AutoDock Vina. MD simulations and trajectory post-processing were executed using the GROMACS 2016.3 software package. Molecular visualizations, hydrogen bond (H-bond) mapping, and structural renderings were generated using PyMOL 3.0, Visual Molecular Dynamics (VMD v.1.9.4), and BIOVIA Discovery Studio Visualizer v.2021. Dynamic analytical plots were produced using QtGrace.

Drug-likeness and toxicity screening

The chemical structures of all 62 compounds retrieved from the literature[13,17,18] were converted to canonical SMILES strings. Pharmacokinetic evaluation was conducted using SwissADME to assess compliance with Lipinski's Rule of Five (RO5), including molecular weight (MW $\leq$ 500 g/mol), octanol-water partition coefficient (LogP $\leq$ 5), hydrogen-bond donors (HBD $\leq$ 5), and hydrogen-bond acceptors (HBA $\leq$ 10). Compounds passing Lipinski's filters were submitted to ProTox-II and ToxTree for computational toxicity assessment, predicting organ toxicities, hepatotoxicity, carcinogenicity, mutagenicity, immunotoxicity, and lethal dose (LD_{50}) classifications.

Ligand and receptor preparation

SMILES strings of selected ligands were converted into 3D atomic coordinates in ChemDraw Professional 18.2 and energy-minimized using the MMFF94 force field. Rotatable bonds were set as flexible to allow full conformational freedom during docking calculations. Receptor preparation involved extracting co-crystallized native ligands, stripping crystallographic

water molecules and heteroatoms, adding polar hydrogen atoms, and assigning partial atomic charges. The modified protein structures were saved in PDBQT format for docking input[19].

Protocol validation and molecular docking

Docking protocols were validated by re-docking the native co-crystallized ligands into their respective binding sites on aldose reductase (3S3G), glucokinase (6E0I), and GSK3-β (1Q5K). Protocol validity was confirmed when the root-mean-square deviation (RMSD) between the re-docked pose and the experimental crystallographic binding mode was ≤ 2.0 Å. Docking calculations were performed using AutoDock Vina, which employs an iterated local-search global optimizer that combines Monte Carlo conformational sampling with the Broyden-Fletcher-Goldfarb-Shanno (BFGS) gradient algorithm. The top 10 binding poses per ligand were generated, and candidate complexes were ranked based on calculated binding affinity energies (kcal/mol).

Molecular dynamics simulations

Unrestrained 100 ns MD simulations were performed for top-ranked protein-ligand complexes using GROMACS 2016.3 under the AMBER ff14SB force field. Ligand topologies and atomic charges were generated using Antechamber with the General AMBER Force Field (GAFF). Each complex was solvated in a cubic box of TIP3P water molecules, maintaining a minimum distance of 1.0 nm between the protein surface and the box edges, and neutralizing counter-ions (Na^+ or Cl^-) were added. Energy minimization was performed using the steepest-descent algorithm for 50,000 steps (emtol < 1000.0 kJ/mol/nm). Systems were equilibrated under an NVT ensemble at 300 K for 100 ps using a modified Berendsen thermostat (V-rescale), followed by NPT equilibration at 1.0 bar for 100 ps using the Parrinello-Rahman barostat. Production MD simulations were executed for 100 ns at 300 K and 1.0 bar with a 2 fs time step. Coordinates were saved every 10 ps for downstream trajectory analysis.

Data analysis

Trajectory coordinates generated during the 100 ns MD simulations were analyzed using built-in GROMACS analysis modules. Structural stability, flexibility, compactness, solvation, and hydrogen-bonding kinetics were quantified using the following analytical tools:

1. gmx rms: RMSD of protein backbone atoms to assess structural stability over time.
2. gmx rmsf: Root-mean-square fluctuation (RMSF) per residue to evaluate local backbone flexibility.
3. gmx gyrate: Radius of gyration (Rg) to assess overall structural compactness.
4. gmx sasa: Solvent-accessible surface area (SASA) to evaluate changes in hydrophilic and hydrophobic exposure.
5. gmx rdf: Radial distribution function (RDF) to determine local solvent structure around active-site complexes.
6. gmx hbond: Intermolecular hydrogen-bond counts and percentage occupancy across the 100 ns trajectory.

Time-series plots were rendered using QtGrace. Binding free energies for top-ranked complexes were calculated using the MM/PBSA method via the g_mmpbsa utility. Calculations were evaluated over 101 snapshot frames extracted at 1 ns intervals from the final steady-state production trajectory (0 to 100 ns). Energy components, including van der Waals, electrostatic, polar solvation, and non-polar solvation energies, were calculated, and statistical uncertainties were determined using 2000 bootstrap iterations (nbs = 2000).

RESULTS AND DISCUSSION

A comprehensive review of the phytochemical constituents of *L. speciosa* identified 62 bioactive compounds. These molecules were initially evaluated for drug-likeness using Lipinski's RO5 via the SwissADME platform. The analysis revealed that 56 compounds complied with RO5 parameters, whereas 6 compounds were excluded due to multiple violations, including MW exceeding 500 Da, MlogP values greater than 4.15, more than 10 hydrogen-bond acceptors, or more than 5 hydrogen-bond donors. Compounds with molecular weights above 500 Da may have difficulty penetrating cell membranes, while an elevated MlogP value indicates poor aqueous solubility[20]. Furthermore, an excessive number of hydrogen-bond donors or acceptors reduces membrane permeability, thereby negatively impacting oral bioavailability[6].

Following drug-likeness screening, the 56 compliant compounds were subjected to toxicological evaluation using the ProTox-II and ToxTree platforms, based on the Cramer Rules and the Kroes Threshold of Toxicological Concern (TTC) decision-tree methods. The Cramer Rules categorize compounds into three classes based on structural complexity and toxicity risk: Class I (simple structures with low oral toxicity), Class II (moderately hazardous compounds), and Class III (structures containing reactive or potentially toxic functional groups)[21]. The Kroes TTC model further refines safety margins by estimating human acceptable daily intake thresholds based on chemical structure[22,23]. Toxicity screening indicated that 42 of the 56 compounds were categorized as safe, as lower toxicity classifications generally present reduced risks of harm upon ingestion[24].

While toxicity screening classified 42 of 56 compounds as safe, several candidates displayed concerning profiles. For example, stigmasterol exhibited immunotoxicity, and gallic acid displayed potential carcinogenicity, underscoring the need for cautious interpretation of *in silico* toxicity predictions. These findings highlight translational limitations, demonstrating that compounds deemed promising computationally may pose safety concerns *in vivo*. To address these limitations, future studies should use structure–activity relationship (SAR) models to guide rational structural optimization, specifically by modifying reactive functional groups to reduce toxicity without compromising therapeutic efficacy.

Before executing large-scale molecular docking simulations, the docking protocol was validated via re-docking. This involved extracting the co-crystallized native ligand from its target protein and re-docking it into the active site. The primary validation parameter was RMSD between crystallographic and re-docked ligand poses, with an RMSD $\leq$ 2.0 Å indicating docking reliability and structural accuracy[25]. The grid box coordinates, generated conformation counts, and RMSD metrics for each target protein are compiled in **Table II**.

Table II. Grid box parameters and native ligand re-docking validation metrics.

Parameter	Aldose reductase (3S3G)	Glucokinase (6E0I)	GSK3-β (1Q5K)
Grid box dimensions (x, y, z)	20 x 20 x 20	30 x 30 x 30	12 x 12 x 12
Grid center coordinates (x, y, z)	(2.577, 7.324, 22.162)	(-9.711, 10.024, -26.887)	(23.148, 22.189, 9.398)
Generated conformations	10	10	10
Re-docked RMSD (Å)	0.4797	0.3278	1.8260
Native binding affinity (kcal/mol)	-12.2	-5.8	-6.9

A total of 42 filtered phytochemicals from *L. speciosa* were docked against aldose reductase, glucokinase, and GSK3-β to identify candidates displaying superior binding affinities relative to native ligands and the clinical metformin control. Outcomes proved highly target-dependent. For aldose reductase, no test compound surpassed the native ligand (-12.2 kcal/mol), although several exceeded the metformin control (-6.2 kcal/mol), with kaempferol demonstrating the strongest affinity (-9.9 kcal/mol). For glucokinase and GSK3-β, the top candidates surpassed both native ligands and control: gallic acid (-7.7 kcal/mol) outperformed the glucokinase native ligand (-5.8 kcal/mol) and metformin (-5.1 kcal/mol), while stigmasterol (-8.9 kcal/mol) outperformed the GSK3-β native ligand (-6.9 kcal/mol) and metformin (-4.7 kcal/mol). These results indicate that while *L. speciosa* phytochemicals do not uniformly surpass native ligands across all targets; they exhibit clear target-specific binding potential while consistently exceeding metformin across all three enzymes. The complete comparative binding dataset is detailed in **Table III**.

Integrating Lipinski's parameters, toxicological profiles, and docking scores identified the top three lead compounds (kaempferol, gallic acid, and stigmasterol) that exhibited favorable ADME profiles and strong target-binding affinities, as summarized in **Table IV** and visualized in **Figure 1**. Kaempferol and gallic acid satisfied all four Lipinski parameters, whereas stigmasterol exceeded the MlogP threshold (6.62 versus the 4.15 cut-off) while complying with the other three criteria. Because Lipinski's RO5 permits a single violation, stigmasterol was retained for further evaluation; nevertheless, this elevated lipophilicity constitutes a drug-likeness limitation that is revisited in the MM/PBSA analysis, where it underlies stigmasterol's predominantly non-specific binding.

Based on docking scores, RO5 compliance, and toxicological profiles, three top-performing complexes were selected for 100 ns MD simulations under physiological conditions: kaempferol bound to aldose reductase, gallic acid bound to glucokinase, and stigmasterol bound to GSK3-β. MD trajectories were evaluated across 100 ns to characterize structural stability, flexibility, solvation parameters, and hydrogen bonding. RMSD quantifies the average positional variance of protein backbone atoms relative to initial reference coordinates, where low RMSD values indicate structural stability and minimal conformational deviation[26].

Table III. Molecular docking binding energies of *L. speciosa* phytochemicals across target proteins.

No.	Compound Name	3S3G (kcal/mol)	6E0I (kcal/mol)	1Q5K (kcal/mol)	Filter Status / Elimination Reason
—	Native ligand	-12.2	-5.8	-6.9	Reference Standard
—	Metformin control	-6.2	-5.1	-4.7	Reference Control
1	γ-Sitosterol	-5.5	-7.1	-8.5	Retained
2	Oleamide	-7.3	-5.1	-5.8	Retained
3	cis-11-Eicosenamide	-7.6	-5.1	-5.8	Retained
4	Hexadecanamide	-7.0	-4.7	-5.6	Retained
5	Octadecanamide	-7.1	-4.7	-5.7	Retained
6	Stigmasterol	-5.8	-7.4	-8.9	Top Candidate (1Q5K)
7	Glycerol β-palmitate	-7.7	-5.6	-5.5	Retained
8	Squalene	-9.1	-6.0	-7.0	Retained
9	*n*-Hexadecanoic acid	-7.1	-4.8	-5.6	Retained
10	Phytol	-7.9	-5.0	-6.0	Retained
11	Campesterol	-6.1	-6.6	-8.5	Retained
12	Vitamin E	-9.5	-6.5	-8.3	Retained
13	Phytol acetate	-8.3	-5.1	-6.4	Retained
14	Ethyl α-D-glucopyranoside	-6.7	-5.6	-4.5	Retained
15	3,7,11,15-Tetramethyl-2-hexadecen-1-ol	-7.6	-5.0	-6.0	Retained
16	1,2,3-Benzenetriol	—	—	—	Eliminated (Toxicity)
17	17-Pentatriacontene	-6.7	-4.1	-4.8	Retained
18	2-Methoxy-4-vinylphenol	-7.1	-5.2	-5.6	Retained
19	Cholesta-4,6-dien-3-ol	-5.6	-6.9	-8.5	Retained
20	1,2-Propanediol	-3.8	-4.1	-2.9	Retained
21	1(10),3-Dien-17-yl acetate	—	—	—	Eliminated (Toxicity)
22	α-Hydroxymyristic acid	-7.2	-5.3	-5.4	Retained
23	Lageracetal	-6.2	-4.4	-4.9	Retained
24	Stigmast-5-en-3-ol oleate	—	—	—	Eliminated (Lipinski)
25	α-Tocopherolquinone	—	—	—	Eliminated (Lipinski)
26	Octadecane	—	—	—	Eliminated (Toxicity)
27	Pentacosane	—	—	—	Eliminated (Toxicity)
28	Dodecane	—	—	—	Eliminated (Toxicity)
29	Tetracosane	—	—	—	Eliminated (Toxicity)
30	Tricosane	—	—	—	Eliminated (Toxicity)
31	Docosane	—	—	—	Eliminated (Toxicity)
32	Neophytadiene	-7.9	-4.9	-6.0	Retained
33	2-Pentadecanone	-6.8	-4.5	-5.3	Retained
34	Heptadecane	—	—	—	Eliminated (Toxicity)
35	Oleic acid	—	—	—	Eliminated (Toxicity)
36	Cyclononanone	-6.8	-5.2	-5.5	Retained
37	9,12-Octadecadienoic acid	-5.3	-4.9	-5.8	Retained
38	Octadecanoic acid	-7.7	-5.0	-5.6	Retained
39	Linolenic acid	-7.0	-5.5	-6.2	Retained
40	Diacetonyl	-7.9	-4.7	-4.3	Retained
41	Stigmastan-3,5-diene	-5.3	-6.4	-7.7	Retained
42	Diamyl phthalate	-5.8	-5.9	-6.3	Retained
43	Cyclononasiloxane	-7.7	-4.3	-2.2	Retained
44	Cyclotetracosane	—	—	—	Eliminated (Toxicity)
45	9,19-Cyclolanostan-3-ol	-5.6	-6.9	-6.5	Retained
46	Z-5-Nonadecene	-7.2	-4.0	-5.3	Retained
47	1-Heneicosyl formate	-7.0	-4.2	-5.5	Retained
48	1-Hexacosanol	-6.9	-4.5	-5.5	Retained
49	Ellagitannin	—	—	—	Eliminated (Lipinski)
50	Stachyurin	—	—	—	Eliminated (Lipinski)
51	2,3-(*S*)-Hexahydroxydiphenoyl-D-glucose	—	—	—	Eliminated (Lipinski)
52	Ellagic acid	—	—	—	Eliminated (Toxicity)
53	Corosolic acid	-4.6	-4.6	-4.6	Retained
54	Gallic acid	-7.2	-7.7	-5.4	Top Candidate (6E0I)
55	4-Hydroxybenzoic acid	-6.9	-6.1	-5.4	Retained
56	Caffeic acid	-8.2	-6.1	-6.1	Retained
57	p-Coumaric acid	-7.8	-5.4	-6.0	Retained
58	Kaempferol	-9.9	-7.1	-8.2	Top Candidate (3S3G)
59	Quercetin	—	—	—	Eliminated (Toxicity)
60	Isoquercitrin	—	—	—	Eliminated (Lipinski)
61	Maslinic acid	-4.4	-4.4	-4.4	Retained
62	Pterocarinin	—	—	—	Eliminated (Toxicity)

Note: Empty entries reflect compound elimination during RO5 or toxicological screening prior to docking.

Table IV. Lipinski's RO5 properties and toxicological profiles of top candidate phytochemicals.

Evaluation Profile	Kaempferol	Gallic Acid	Stigmasterol
Molecular weight (<500 g/mol)	286.24	170.12	412.69
H-Bond donors (<5)	4	4	1
H-Bond acceptors (<10)	6	5	1
mLogP (<4.15)	-0.03	-0.16	6.62
LD_{50} (mg/kg)	3919	2000	890
Toxicity endpoints	Inactive	Carcinogenicity Active (P: 0.56)	Immunotoxicity Active (P: 0.99)
Cramer rules	High (Class III)	Low (Class I)	High (Class III)
Kroes TTC	Safe	Safe	Safe
Target receptor	Aldose Reductase	Glucokinase	GSK3-β
Binding affinity (kcal/mol)	-9.9	-7.7	-8.9

Note: P = calculated probability.

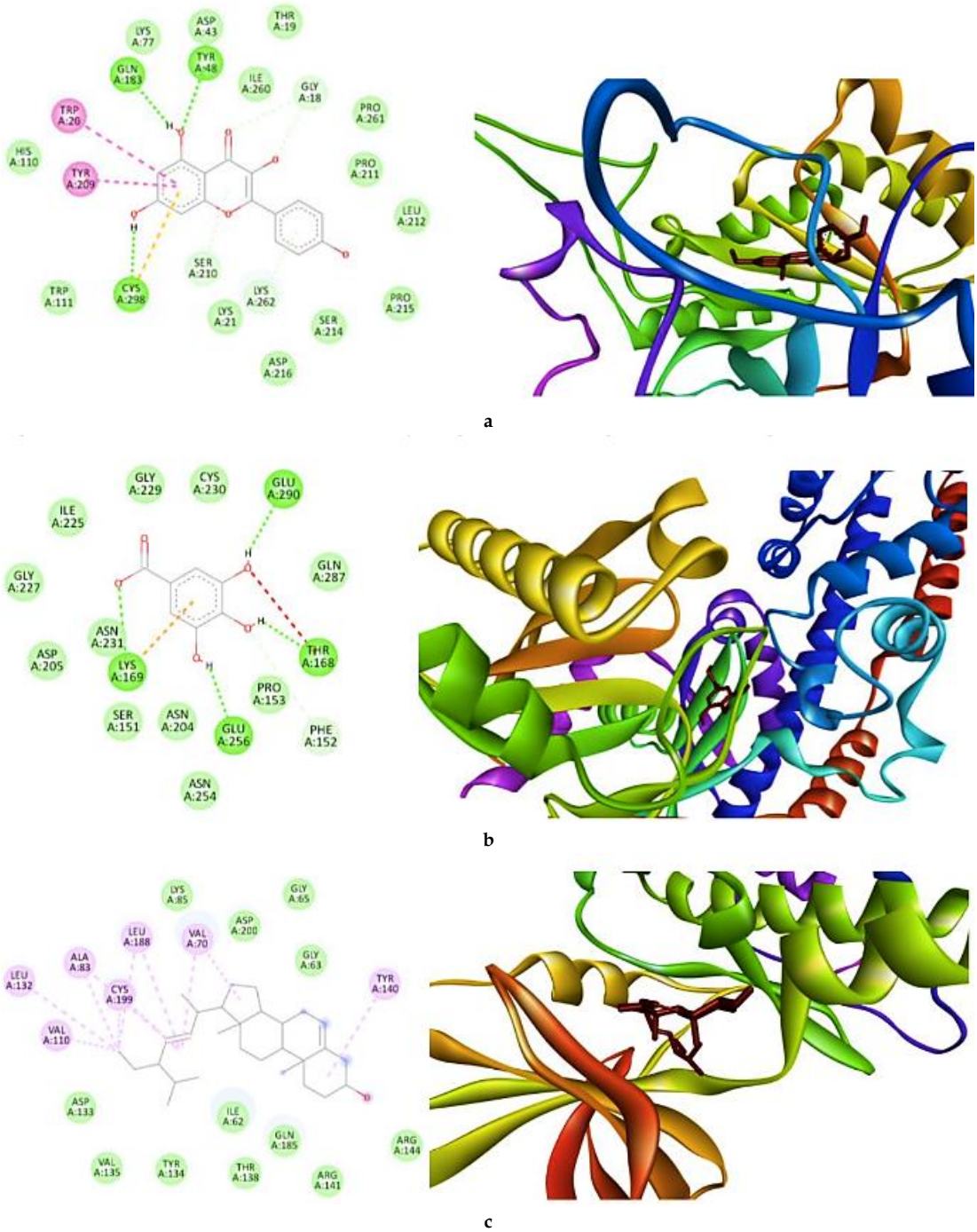

Figure 1. Molecular docking interaction visualizations: (**a**) Aldose reductase–kaempferol complex (3S3G); (**b**) Glucokinase–gallic acid complex (6E0I); (**c**) GSK3-β–stigmasterol complex (1Q5K).

RMSD analysis (**Figure 2**) showed that all three complexes remained stable over the initial 60 ns of the simulation, with RMSD values below 0.25 nm. Beyond 60 ns, gallic acid exhibited pronounced RMSD fluctuations, reaching up to 0.35 nm, likely due to its smaller molecular weight and greater flexibility, which permit increased mobility within the binding pocket. In contrast, kaempferol and stigmasterol maintained stable RMSD trajectories with less than 0.20 nm variation after 60 ns, indicating sustained positional retention within active sites[27].

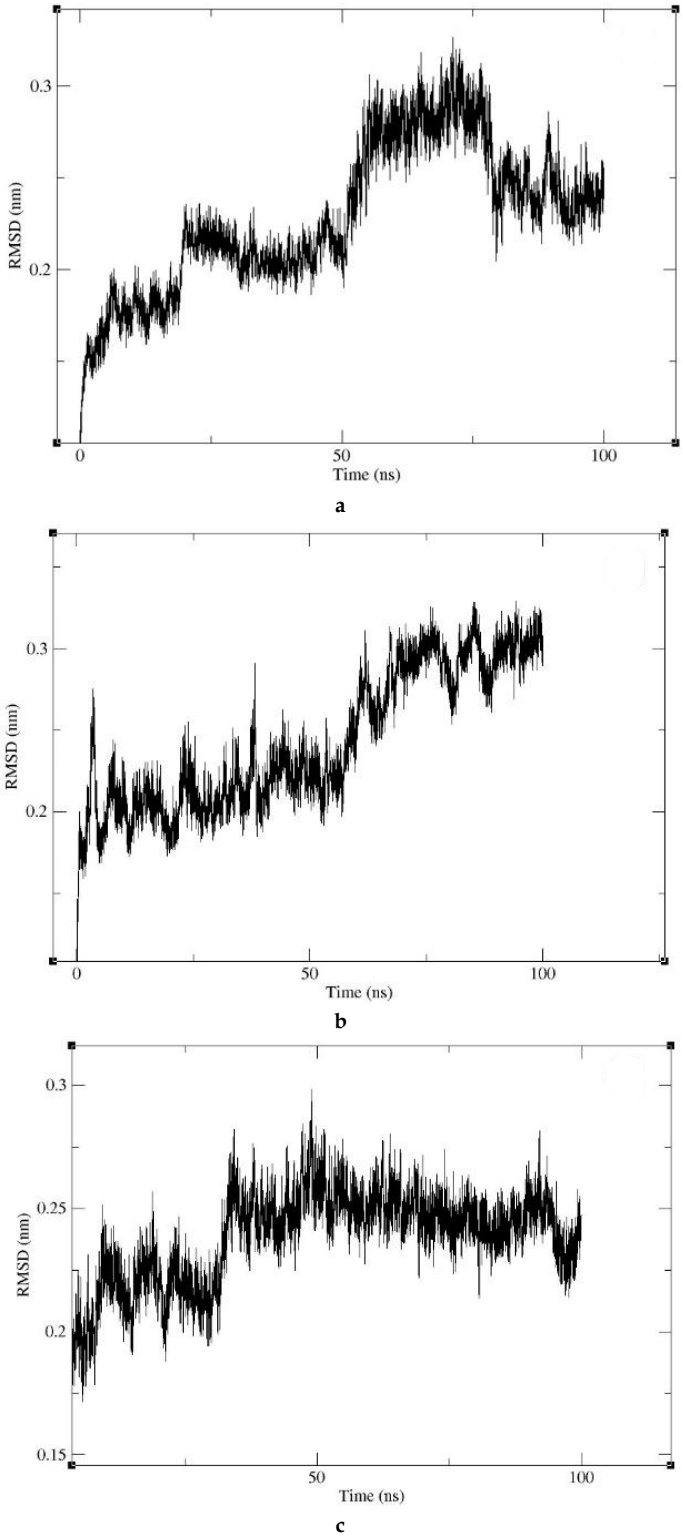

Figure 2. Backbone RMSD trajectories over 100 ns: (**a**) Aldose reductase-kaempferol; (**b**) Glucokinase-gallic acid; (**c**) GSK3-β-stigmasterol.

RMSF measures residue-specific positional deviations, providing insight into local backbone flexibility. High RMSF values indicate dynamic loops or flexible regions, whereas low values indicate rigid structural elements[28]. RMSF analysis (**Figure 3**) revealed distinct residue-level dynamics. The stigmasterol complex exhibited the highest RMSF values, particularly in loop regions near the active site, reflecting weaker, transient interactions. These fluctuations suggest that stigmasterol's bulky sterol framework induces local structural adjustments. In contrast, the gallic acid complex displayed consistently low RMSF values across most residues, indicating limited structural perturbation and a rigid protein interface despite the ligand's internal flexibility. Kaempferol showed moderate fluctuations localized near active-site loops, representing structural adaptations to accommodate the ligand[29].

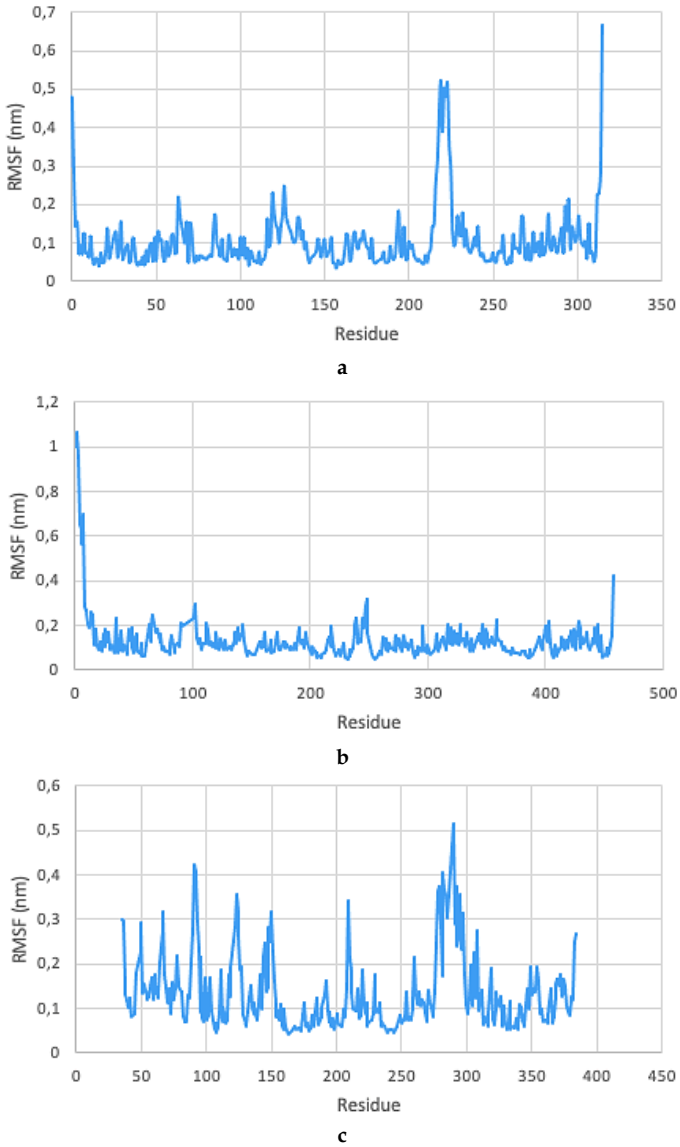

Figure 3. Residue-Level RMSF Profiles: Comparison across (**a**) kaempferol, (**b**) gallic acid, and (**c**) stigmasterol complexes.

SASA quantifies the solvent-exposed surface area of biomolecular complexes, with stable values indicating preserved tertiary structure without large-scale unfolding or compaction. SASA profiles (**Figure 4**) remained stable across all three complexes throughout the 100 ns simulation. Constant SASA values confirm that the proteins retained compact tertiary structures without major unfolding[30]. Gallic acid maintained the lowest SASA profile (~140 nm^2), consistent with its small molecular footprint. Kaempferol (~155 nm^2) and stigmasterol (~165 nm^2) displayed slightly higher but stable SASA profiles, confirming that all three ligands remained securely bound within their pockets without inducing structural exposure[31].

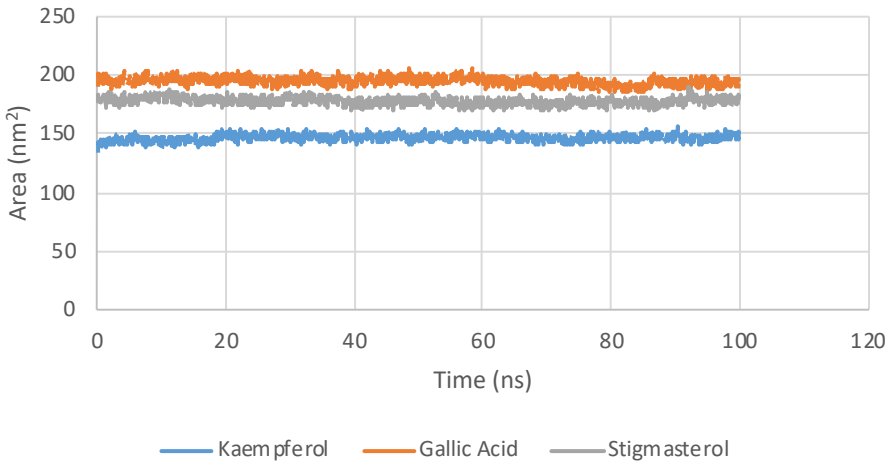

Figure 4. SASA trajectories for target complexes.

The Rg assesses the overall compactness and structural integrity of protein-ligand complexes[32]. Rg analysis (**Figure 5**) showed that all three systems maintained stable structural compactness over 100 ns. Gallic acid exhibited the highest Rg values (~2.4 nm) with minimal variance, indicating a stable, slightly expanded complex. Kaempferol exhibited the lowest and most stable Rg value (~1.9 nm), indicating a tightly packed complex. Stigmasterol maintained intermediate Rg values (~2.1 nm) with minor fluctuations due to its bulky framework. These trends align with SASA and RMSD data, reinforcing that no unfolding occurred during the simulation[33].

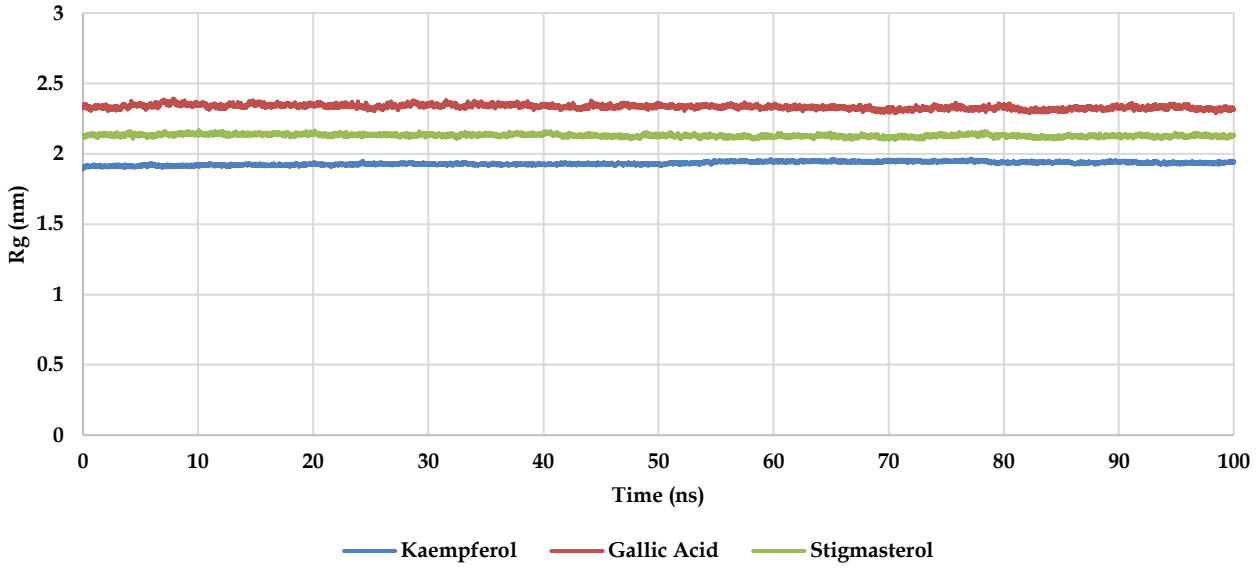

Figure 5. Rg Trajectories over 100 ns.

RDF quantifies the probability of finding surrounding atoms at specific radial distances from ligand atoms, with sharp peaks indicating tight, localized interactions[34]. As shown in **Figure 6**, stigmasterol exhibited a broad, gradual RDF curve, indicating diffuse, nonspecific atomic packing attributable to its bulky hydrophobic structure. Conversely, kaempferol and gallic acid exhibited sharp RDF peaks centered at 0.6–0.8 nm, confirming specific, highly localized atomic interactions[35].

Hydrogen bond occupancy measures the percentage of simulation time during which a specific H-bond remains formed, serving as a key metric of interaction stability[36]. As detailed in **Table V**, kaempferol demonstrated high H-bond occupancy (64.38%), forming persistent directional interactions with key active-site residues. In contrast, stigmasterol exhibited minimal H-bond occupancy (4.24%), reflecting its reliance on non-specific hydrophobic contact rather than localized polar bonding[37].

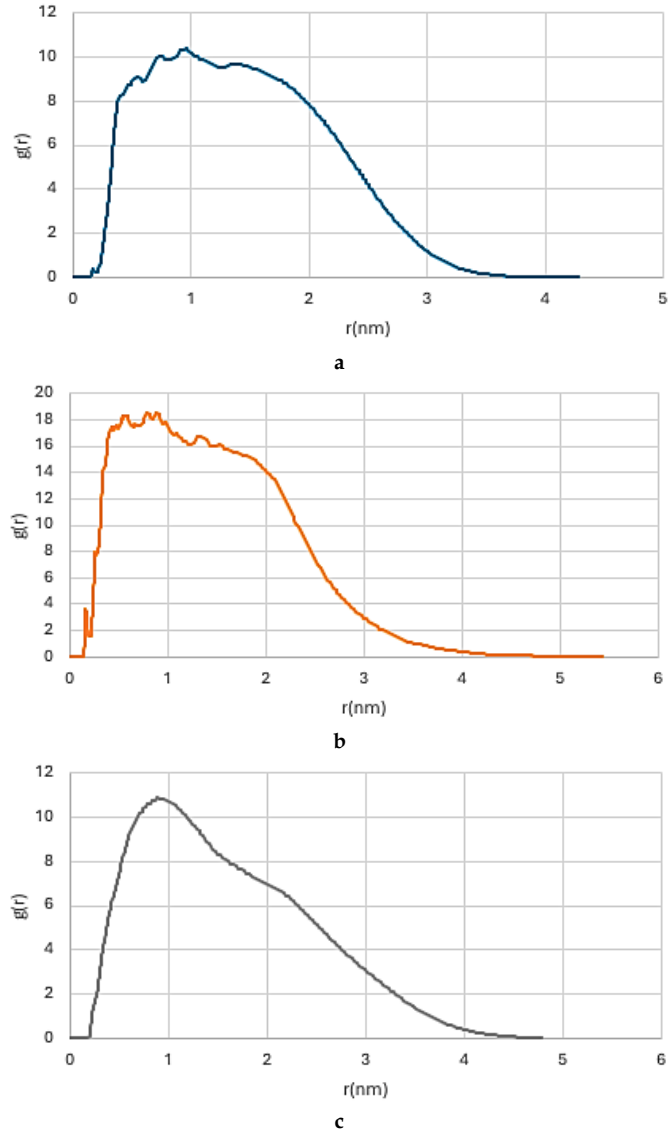

Figure 6. RDF profiles for (**a**) kaempferol, (**b**) gallic acid, and (**c**) stigmasterol complexes.

Table V. Intermolecular H-bond occupancy across simulation trajectories.

Complex System	Target Protein	H-Bond Occupancy (%)	Interaction Characteristic
Kaempferol	Aldose reductase	64.38	Highly persistent & specific
Stigmasterol	GSK3-β	4.24	Intermittent & non-specific

Binding free energies calculated via the MM/PBSA method[38] are presented in **Table VI**. The calculated MM/PBSA binding free energies ($\Delta G_{binding}$) were -65.714 ± 1.45 kJ/mol for kaempferol, -45.629 ± 1.38 kJ/mol for gallic acid, and -133.377 ± 1.62 kJ/mol for stigmasterol. Although stigmasterol yielded the most negative total binding energy, energy decomposition reveals that this driven score stems almost entirely from non-specific van der Waals interactions (E_{vdW} = -181.809 kJ/mol vs. E_{elec} = -9.647 kJ/mol), accounting for ~95% of its total attractive force. This non-specific hydrophobic burial is corroborated by MD trajectories showing low H-bond occupancy (4.24%), a diffuse RDF profile, and elevated active-site RMSF. Conversely, kaempferol exhibited a balanced energy profile, with electrostatic contributions (E_{elec} = -41.072 kJ/mol) accounting for ~21% of the total attractive forces, four times that of stigmasterol. This aligns with kaempferol's high H-bond occupancy (64.38%), sharp RDF peaks, and compact Rg profile (~1.9 nm). Gallic acid was electrostatically dominated (E_{elec} = -206.744 kJ/mol, ~73% of attractive terms), reflecting its polar structure. Furthermore, stigmasterol's favorable binding score is offset by its Lipinski violation (MlogP = 6.62) and predicted immunotoxicity. Consequently, kaempferol is the premier drug-like lead candidate for aldose reductase inhibition, with gallic acid serving as a complementary, target-specific lead for glucokinase.

Table VI. MM/PBSA binding free energy components for top candidate complexes.

Complex System	E_{elec} (kJ/mol)	E_{vdW} (kJ/mol)	G_{polar} (kJ/mol)	$G_{nonpolar}$ (kJ/mol)	$\Delta G_{binding}$ (kJ/mol)
Kaempferol	-41.072 ± 0.85	-158.760 ± 1.12	148.851 ± 1.05	-14.733 ± 0.42	-65.714 ± 1.45
Gallic acid	-206.744 ± 1.22	-77.558 ± 0.94	247.961 ± 1.18	-9.288 ± 0.31	-45.629 ± 1.38
Stigmasterol	-9.647 ± 0.45	-181.809 ± 1.35	78.811 ± 0.88	-20.733 ± 0.51	-133.377 ± 1.62

These findings align with prior computational studies on flavonoid aldose reductase inhibitors. Yasir *et al*.[39] similarly identified kaempferol as a top-ranked aldose reductase inhibitor using an analogous docking–MD–MM/PBSA workflow, a finding supported experimentally by *in vitro* assays demonstrating an IC_{50} of 0.02 uM[40]. By identifying kaempferol, gallic acid, and stigmasterol, this study expands the recognized antidiabetic potential of *L. speciosa* beyond corosolic acid.

CONCLUSION

This study successfully addressed the critical research gap surrounding *L. speciosa* by moving beyond its extensively studied constituent, corosolic acid, and conducting a comprehensive *in silico* evaluation of 62 phytochemicals derived from the plant. Through molecular docking targeting three key antidiabetic enzymes, kaempferol, gallic acid, and stigmasterol were identified as the top-performing candidate ligands for aldose reductase, glucokinase, and GSK3-β, respectively. Subsequent MD simulations and trajectory analyzes confirmed that all three complexes remained structurally stable under physiological conditions while exhibiting distinct differences in interaction specificity. Furthermore, MM/PBSA binding free energy calculations revealed that although stigmasterol achieved the lowest binding energy (-133.377 ± 1.62 kJ/mol), its binding was dominated by nonspecific van der Waals interactions and low hydrogen-bond occupancy. Conversely, kaempferol exhibited a balanced energy profile and the highest hydrogen-bond occupancy, thereby establishing persistent, directional, and selective binding to aldose reductase. When integrated with ADME and toxicity evaluations, which highlighted immunotoxicity and lipophilicity violations in stigmasterol, kaempferol emerged as the premier stable, selective, and drug-like lead candidate for antidiabetic therapy. These findings provide a solid computational foundation validating *L. speciosa* as a valuable source of multi-target antidiabetic agents and warrant further *in vitro* and *in vivo* experimental investigation.

ACKNOWLEDGMENT

The authors express their sincere gratitude to Universitas Lambung Mangkurat for providing financial support for this study through the Universitas Lambung Mangkurat Research Grant for the 2024 fiscal year (Grant No. 1374.5/UN8.2/PG/2024).

AUTHORS' CONTRIBUTION

Conceptualization: Aditya Maulana Perdana Putra
Data curation: Aditya Maulana Perdana Putra, Khoirunnisa Muslimawati, Normaidah, Putri Helena Junjung Buih
Formal analysis: Aditya Maulana Perdana Putra, Nabila Hadiah Akbar, Catherina Adeline Kurniawan
Funding acquisition: Aditya Maulana Perdana Putra
Investigation: Aditya Maulana Perdana Putra, Anna Khumaira Sari, Okta Muthia Sari
Methodology: Khorunnisa Muslimawati, Normaidah, Catherina Adeline Kurniawan
Project administration: Dita Ayulia Dwisandi, Anna Khumaira Sari, Putri Helena Junjung Buih
Resources: -
Software: Khorunnisa Muslimawati, Normaidah, Catherina Adeline Kurniawan
Supervision: Normaidah, Anna Khumaira Sari, Ariranur Haniffadli
Validation: Normaidah, Anna Khumaira Sari, Ariranur Haniffadli
Visualization: Aditya Maulana Perdana Putra, Khoirunnisa Muslimawati
Writing - original draft: Aditya Maulana Perdana Putra, Nabila Hadiah Akbar, Okta Muthia Sari
Writing - review & editing: Khoirunnisa Muslimawati, Nabila Hadiah Akbar, Dita Ayulia Dwisandi, Ariranur Haniffadli

DATA AVAILABILITY

All data are available on request from the corresponding author.

CONFLICT OF INTEREST

The authors declare no conflicts of interest related to this study.

REFERENCES

1. Hossain MJ, Al-Mamun M, Islam MR. Diabetes mellitus, the fastest growing global public health concern: Early detection should be focused. Health Sci Rep. 2024;7(3):e2004. DOI: 10.1002/hsr2.2004; PMID: 38524769; PMCID: PMC10958528.

2. Adnan Y, Hadju V, Mallongi A, Ali MSS. The Economic Cost of Type 2 Diabetes in Indonesia: A Systematic Review. Iran J Public Health. 2025;54(10):2139-50. DOI: 10.18502/ijph.v54i10.20118; PMID: 41357699; PMCID: PMC12675950.

3. Ryszkiewicz P, Malinowska B, Schlicker E. Polypharmacology: new drugs in 2023-2024. Pharmacol Rep. 2025;77(3):543-60. DOI: 10.1007/s43440-025-00715-8; PMID: 40095348; PMCID: PMC12066383.

4. Polonsky WH, Henry RR. Poor medication adherence in type 2 diabetes: recognizing the scope of the problem and its key contributors. Patient Prefer Adherence. 2016;10:1299-307. DOI: 10.2147/PPA.S106821; PMID: 27524885; PMCID: PMC4966497.

5. Coimbra JTS, Feghali R, Ribeiro RP, Ramos MJ, Fernandes PA. The importance of intramolecular hydrogen bonds on the translocation of the small drug piracetam through a lipid bilayer. RSC Adv. 2021;11(2):899-908. DOI: 10.1039/d0ra09995c; PMID: 35423709; PMCID: PMC8693363.

6. Lin A, Zhang Z, Jiang A, Li K, Shi Y, Yang H, et al. Computational approaches to druggable site identification: Current status and future perspective. Acta Pharm Sin B. 2026;16(1):62-92. DOI: 10.1016/j.apsb.2025.10.032; PMID: 41584329; PMCID: PMC12827903.

7. Arif R, Ahmad S, Mustafa G, Mahrosh HS, Ali M, Qamar MTU, et al. Molecular Docking and Simulation Studies of Antidiabetic Agents Devised from Hypoglycemic Polypeptide-P of Momordica charantia. Biomed Res Int. 2021;2021:5561129. DOI: 10.1155/2021/5561129; PMID: 34589547; PMCID: PMC8476269.

8. Singh M, Kapoor A, Bhatnagar A. Physiological and Pathological Roles of Aldose Reductase. Metabolites. 2021;11(10):655. DOI: 10.3390/metabo11100655; PMID: 34677370; PMCID: PMC8541668.

9. Aqel YA, Alnesf A, Aigha II, Islam Z, Kolatkar PR, Teo A, et al. Glucokinase (GCK) in diabetes: from molecular mechanisms to disease pathogenesis. Cell Mol Biol Lett. 2024;29(1):120. DOI: 10.1186/s11658-024-00640-3; PMID: 39245718; PMCID: PMC11382428.

10. Wang L, Li J, Di LJ. Glycogen synthesis and beyond, a comprehensive review of GSK3 as a key regulator of metabolic pathways and a therapeutic target for treating metabolic diseases. Med Res Rev. 2022;42(2):946-82. DOI: 10.1002/med.21867; PMID: 34729791; PMCID: PMC9298385.

11. Yue Z, Xu Y, Cai M, Fan X, Pan H, Zhang D, Zhang Q. Floral Elegance Meets Medicinal Marvels: Traditional Uses, Phytochemistry, and Pharmacology of the Genus Lagerstroemia L. Plants. 2024;13(21):3016. DOI: 10.3390/plants13213016; PMID: 39519935; PMCID: PMC11548200.

12. Sonar MP, Rathod VK. Extraction of type II antidiabetic compound corosolic acid from Lagerstroemia speciosa by batch extraction and three phase partitioning. Biocatal Agric Biotechnol. 2020;27:101694. DOI: 10.1016/j.bcab.2020.101694.

13. Sirikhansaeng P, Tanee T, Sudmoon R, Chaveerach A. Major Phytochemical as γ-Sitosterol Disclosing and Toxicity Testing in Lagerstroemia Species. Evid Based Complement Alternat Med. 2017;2017:7209851. DOI: 10.1155/2017/7209851; PMID: 28191023; PMCID: PMC5278189.

14. Yin B, Bi YM, Fan GJ, Xia YQ. Molecular Mechanism of the Effect of Huanglian Jiedu Decoction on Type 2 Diabetes Mellitus Based on Network Pharmacology and Molecular Docking. J Diabetes Res. 2020;2020:5273914. DOI: 10.1155/2020/5273914; PMID: 33134394; PMCID: PMC7593729.

15. Venkateswarulu TC, Vajiha, Krupanidhi S, Mikkili I, Angelina J, Babu DJ, et al. In silico study on evaluation of corosolic acid of Lagerstroemia speciosa against Alzheimer's disease. Arab Gulf Journal of Scientific Research. 2023;41(2):175–82. DOI: 10.1108/AGJSR-04-2022-0039.

16. Chandran M, George S, Santhalingam K, Gangwar P, Krishnakumar K. Molecular docking Studies of 2α-Hydroxyursolic acid derivatives for hypercholesterolemia. Int J PharmTech Res. 2011;3(3):1576-81.

17. Choi JS, Ku PT, Cho KS, Huh MK. Comparison of Chemicals in Lagerstroemia speciosa (L.) Pers. at Growing Stage Levels by GC-MS. Korean J Crop Sci. 2010;55(3):200-6.

18. Al-Snafi AE. Medicinal Value of Lagerstroemia speciosa: An Updated Review. Int J Curr Pharm Res. 2019;11(5):18–26. DOI: 10.22159/ijcpr.2019v11i5.35708.

19. Pratama MRF, Praditapuspa EN, Kesuma D, Poerwono H, Widiandani T, Siswodihardjo S. Boesenbergia Pandurata as an Anti-Breast Cancer Agent: Molecular Docking and ADMET Study. Lett Drug Des Discov. 2022;19(7):606-26. DOI: 10.2174/1570180819666211220111245.

20. Wu K, Kwon SH, Zhou X, Fuller C, Wang X, Vadgama J, et al. Overcoming Challenges in Small-Molecule Drug Bioavailability: A Review of Key Factors and Approaches. Int J Mol Sci. 2024;25(23):13121. DOI: 10.3390/ijms252313121; PMID: 39684832; PMCID: PMC11642056.

21. EFSA Scientific Committee; More SJ, Bampidis V, Benford D, Bragard C, Halldorsson TI, et al. Guidance on the use of the Threshold of Toxicological Concern approach in food safety assessment. EFSA J. 2019;17(6):e05708. DOI: 10.2903/j.efsa.2019.5708; PMID: 32626331; PMCID: PMC7009090.

22. Kroes R, Renwick AG, Cheeseman M, Kleiner J, Mangelsdorf I, Piersma A, et al. Structure-based thresholds of toxicological concern (TTC): guidance for application to substances present at low levels in the diet. Food Chem Toxicol. 2004;42(1):65-83. DOI: 10.1016/j.fct.2003.08.006; PMID: 14630131.

23. Yamada T, Kurimoto M, Hirose A, Yang C, Rathman JF. Development of a New Threshold of Toxicological Concern Database of Non-cancer Toxicity Endpoints for Industrial Chemicals. Front Toxicol. 2021;3:626543. DOI: 10.3389/ftox.2021.626543; PMID: 35295111; PMCID: PMC8915903.

24. Jurowski K, Krośniak A. Prediction of key toxicity endpoints of AP-238 a new psychoactive substance for clinical toxicology and forensic purposes using in silico methods. Sci Rep. 2024;14(1):28977. DOI: 10.1038/s41598-024-79453-5; PMID: 39578526; PMCID: PMC11584713.

25. Shen T, Shen H, Kong Y, Qiang W, Yu X, Wang J. Structure-based virtual screening identifies novel small-molecule inhibitors targeting the endonuclease active site of APE1. Sci Rep. 2026;16(1):21299. DOI: 10.1038/s41598-026-51975-0; PMID: 42106528; PMCID: PMC13346695.

26. Xiong C, Kandhan P, Chen D, Ma Z, Smith ED, Tao P. Efficient Sampling of Short Protein Trajectories with Conditional Diffusion Models. J Chem Theory Comput. 2026;22(1):78-94. DOI: 10.1021/acs.jctc.5c01579; PMID: 41481844; PMCID: PMC12861079.

27. Makeneni S, Thieker DF, Woods RJ. Applying Pose Clustering and MD Simulations To Eliminate False Positives in Molecular Docking. J Chem Inf Model. 2018;58(3):605-14. DOI: 10.1021/acs.jcim.7b00588; PMID: 29431438; PMCID: PMC6067002.

28. Nettey-Oppong EE, Muhammad R, Ali A, Jeong HW, Seok YS, Kim SW, et al. The Impact of Temperature and Pressure on the Structural Stability of Solvated Solid-State Conformations of Bombyx mori Silk Fibroins: Insights from Molecular Dynamics Simulations. Materials. 2024;17(23):5686. DOI: 10.3390/ma17235686; PMID: 39685120; PMCID: PMC11642577.

29. Calderon A, Harbinson E, Ettrich R, Kulik N, Carey J. An MD View of Ligand Binding. Molecules. 2025;30(24):4678. DOI: 10.3390/molecules30244678; PMID: 41471704; PMCID: PMC12736043.

30. Cao X, Hummel MH, Wang Y, Simmerling C, Coutsias EA. Exact Analytical Algorithm for the Solvent-Accessible Surface Area and Derivatives in Implicit Solvent Molecular Simulations on GPUs. J Chem Theory Comput. 2024;20(11):4456-68. DOI: 10.1021/acs.jctc.3c01366; PMID: 38780181; PMCID: PMC11530138.

31. Wang Y, Zhou Y, Khan FI. Molecular Insights into Structural Dynamics and Binding Interactions of Selected Inhibitors Targeting SARS-CoV-2 Main Protease. Int J Mol Sci. 2024;25(24):13482. DOI: 10.3390/ijms252413482; PMID: 39769245; PMCID: PMC11677904.

32. Tanner JJ. Empirical power laws for the radii of gyration of protein oligomers. Acta Crystallogr D Struct Biol. 2016;72(Pt 10):1119-29. DOI: 10.1107/S2059798316013218; PMID: 27710933; PMCID: PMC5053138.

33. Anand AA, Anwar S, Yadav V, Samanta SK. A comparative study of computational modeling approaches for evaluating structural dynamics and algorithmic suitability of short length peptides. Sci Rep. 2025;15(1):34351. DOI: 10.1038/s41598-025-16866-w; PMID: 41038912; PMCID: PMC12491430.

34. de Freitas RF, Schapira M. A systematic analysis of atomic protein-ligand interactions in the PDB. Medchemcomm. 2017;8(10):1970-81. DOI: 10.1039/c7md00381a; PMID: 29308120; PMCID: PMC5708362.

35. Goharshadi EK. A review on the radial distribution function: Insights into molecular structure, intermolecular interactions, and thermodynamic properties. J Mol Liq. 2025;433:127900. DOI: 10.1016/j.molliq.2025.127900.

36. Swiatla-Wojcik D. Simulation Studies of the Dynamics and the Connectivity Patterns of Hydrogen Bonds in Water from Ambient to Supercritical Conditions. Molecules. 2024;29(23):5513. DOI: 10.3390/molecules29235513; PMID: 39683673; PMCID: PMC11644018.

37. Bertalan É, Konno M, Marín MDC, Bagherzadeh R, Nagata T, Brown L, et al. Hydrogen-Bonding and Hydrophobic Interaction Networks as Structural Determinants of Microbial Rhodopsin Function. J Phys Chem B. 2024;128(30):7407-26. DOI: 10.1021/acs.jpcb.4c02946; PMID: 39024507.

38. Wang C, Greene D, Xiao L, Qi R, Luo R. Recent Developments and Applications of the MMPBSA Method. Front Mol Biosci. 2018;4:87. DOI: 10.3389/fmolb.2017.00087; PMID: 29367919; PMCID: PMC5768160.

39. Yasir M, Park J, Han ET, Han JH, Park WS, Chun W. Investigating the Inhibitory Potential of Flavonoids against Aldose Reductase: Insights from Molecular Docking, Dynamics Simulations, and gmx_MMPBSA Analysis. Curr Issues Mol Biol. 2024;46(10):11503-18. DOI: 10.3390/cimb46100683; PMID: 39451563; PMCID: PMC11506312.

40. Quilantang NG, Limbo CA, Lee JS, Jacinto SD, Moon SK, Lee S. Aldose reductase inhibition of Rosa hybrida petals and its active component, kaempferol. Hortic Environ Biotechnol. 2020;61:601–7. DOI: 10.1007/s13580-020-00232-y.